Journal of Basic Physical Research ISSN: 2141-8403 Prints, 2141-8411 Online
Vol.15, Issue 1, March, 2026, pp. 107– 113, Available online at https://journals.unizik.edu.ng/jbpr/

ENGINEERING OPTO-ELECTRONIC PROPERTIES OF CUO-ZNO NANOCOMPOSITE THIN FILMS FOR DUAL-FUNCTIONAL APPLICATIONS IN PHOTOVOLTAICS AND PHOTOCATALYSIS

Ikenga Onyeka Anthony [1] [*]; Nwaneri, Israel Nzoputa[1]; Emeremogonu, Christian Chinedu[2]; Isi, Pretty O.[1], Alor, Kenechukwu Perpetua[1]; Nwankwo, Elizabeth Uzoamaka.[1]
[1]Nnamdi Azikiwe University, Awka, Nigeria, [2]University of Maryland, Baltimore County, USA.

Abstract
The opto-electronic properties of metal oxide nanocomposites are highly tunable through compositional control, enabling their application across diverse fields. This study presents a facile chemical bath deposition method to fabricate CuO-ZnO thin films with varying precursor concentrations (0.2M - 0.8M). UV-Vis spectroscopy revealed that the optical bandgap could be engineered from 3.5eV down to 2.2eV, with the 0.4M concentration exhibiting optimal characteristics: the narrowest bandgap, highest absorbance across the visible spectrum, and favourable film thickness. These properties are critically dissected for two key applications. The enhanced visible light absorption and ideal band alignment suggest superior performance as a photoactive layer in low-cost photovoltaic cells. Concurrently, the narrow bandgap and promoted charge separation at the CuO-ZnO p-n junction position this same 0.4M film as an efficient visible-light-driven photocatalyst for environmental remediation. This work demonstrates the successful design of a single, versatile nanomaterial with high potential for advancing both clean energy generation and water purification technologies.
Keywords: *CuO-ZnO Nanocomposite, Band Gap Engineering, Chemical Bath Deposition, Thin Films, Photovoltaics, Photocatalysis, Solar Energy, Water Treatment.*

Introduction

Imagine being able to design a material from the ground up to perfectly capture sunlight or efficiently drive a chemical reaction with that same light. That's the promise of metal oxide semiconductors, and it's why they've become the darlings of modern materials science. They are the quiet workhorses behind our LEDs, solar cells, and even the tiny photodetectors in our devices (Kuo et al., 2013). On its own, Zinc Oxide (ZnO) is a fantastic material. Think of it as a reliable, wide-bandgap semiconductor (about 3.37 eV) that's naturally an n-type, meaning its primary charge carriers are electrons. It's particularly good at interacting with high-energy UV light (Özgür et al., 2005). On the other hand, Copper Oxide (CuO) is its complementary partner. It's a p-type semiconductor (with positive "holes" as its main carriers) and has a much narrower bandgap (1.2-1.9 eV). This allows it to tango beautifully with visible light, but it's not the best conductor (Volanti et al., 2013). By blending ZnO and CuO into a composite, we can create a "p-n junction" at the nanoscale, which helps separate electrical charges more effectively. This partnership helps overcome their individual weaknesses and creates something far more powerful than the sum of its parts. The key to unlocking this potential lies in the blend ratio. The relative amounts of CuO and ZnO don't just change the chemistry; they fundamentally alter the material's microstructure and, consequently, its interaction with light and electricity (Borkar et al., 2016).

This ability to dial in specific properties by simply varying the composition is what makes binary metal oxide blends like CuO-ZnO so exciting (Dong et al., 2015). Researchers have been diligently mapping out this behavior. For instance, Wang et al. (2011) found that as they increased the amount of CuO in electrodeposited films, the bandgap shrank in a predictable way, from 3.02 eV down to 1.62 eV. This shrinking act is often due to the CuO influencing the electronic structure of ZnO. Similarly, Sue et al. (2010) saw this same trend in nanoparticles made with a sol-gel method, with the bandgap sliding from 3.29 eV (pure ZnO) to 1.62 eV (pure CuO). But it's not just about the bandgap. He et al. (2011) discovered that

there's a "sweet spot" for electrical conductivity in their nanofiber mats—it peaked at just 2% CuO before dropping off, suggesting that too much of a good thing can disrupt the flow of electricity. Vinodkumar et al. (2013) used photoluminescence spectroscopy to show that adding even a tiny amount of CuO (up to 1 wt%) progressively quenched the characteristic UV light emission from ZnO. This is fantastic news for solar cells and photocatalysis, as it means the excited electrons aren't wasting their energy by re-emitting light. Instead, they're being efficiently separated at the ZnO-CuO junction, ready to do useful work.

Methodology

Our goal was to see this tuning in action. We prepared four different samples, which we simply called Slides 1 through 4. Each started with a 10ml solution of CuO and 10ml of ZnO at matching concentrations. For Slide 1, we used 0.2M solutions of each. For Slide 2, 0.4M; Slide 3, 0.6M; and Slide 4, 0.8M. We mixed them thoroughly in a small beaker to create a homogenous blend. To ensure the chemical reaction would proceed correctly, we used triethanolamine (TEA) to carefully adjust and stabilize the pH of each mixture to around 8.7. Slide 1, 2, 3 and 4 was allowed to deposit for 60 minutes respectively and then oven- dried.

After the chemical bath deposition, we had beautiful, thin films coating our glass substrates. To understand their optical personality, we used a UV-Visible spectrophotometer. This instrument measures how much light the film absorbs and transmits at each wavelength, giving us the data we need to calculate key properties like film thickness and, most importantly, the band gap.

Results and Discussion

Optical Analysis of ZNO/CUO Blend

We analyzed all four films across the UV and visible spectrum (200–800nm). The story that emerged from the data was clear: concentration is the master dial for controlling their properties.

Absorption Spectra

The absorption spectra of CuO-ZnO is displayed in figure 3.1 below.

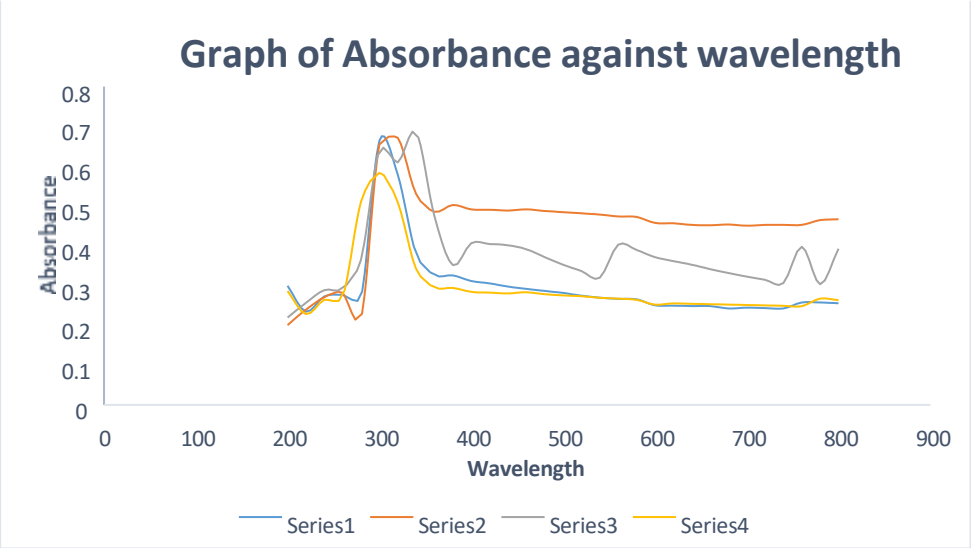


Fig 3.1: Absorbance versus wavelength for CuO-ZnO nanocomposite thin films prepared at different precursor concentration (0.2M – 0.8M)

The absorption spectra reveal a distinct concentration-dependent optical behavior across the UV-Vis region (200-800 nm). All films exhibit relatively low absorbance in the UV region (below 400 nm), with absorption increasing markedly as the wavelength extends into the visible spectrum. This trend is characteristic of metal oxide semiconductors and indicates the successful incorporation of CuO, which extends the light absorption capability of ZnO from the UV into the visible range.

Slide 2 (0.4M) demonstrates superior optical absorption, achieving peak absorbance values approaching 0.75 a.u. in the visible region. This enhanced photon capturing capability can be attributed to favorable film thickness (~1100 nm) that provides sufficient optical path length for photon-material interaction. The high absorbance suggests efficient light harvesting, which is fundamental for both photovoltaic and photocatalytic applications. Slide 3 (0.6M) shows intermediate absorbance (~0.4-0.5 a.u.), while Slides 1 (0.2M) and 4 (0.8M) exhibit the lowest absorbance values (<0.3 a.u.). The non-monotonic trend where absorbance increases from 0.2M to 0.4M, then decreases at higher concentrations is particularly significant. This behavior indicates that beyond an optimal concentration threshold (0.4M), excessive CuO incorporation may lead to Agglomeration of nanoparticles, reducing effective surface area.

The superior absorbance of Slide 2 validates the hypothesis that intermediate compositions achieve the most favorable microstructure for light interaction, balancing the wide-bandgap UV-absorbing ZnO with the visible-light-absorbing CuO.

Transmission Spectra

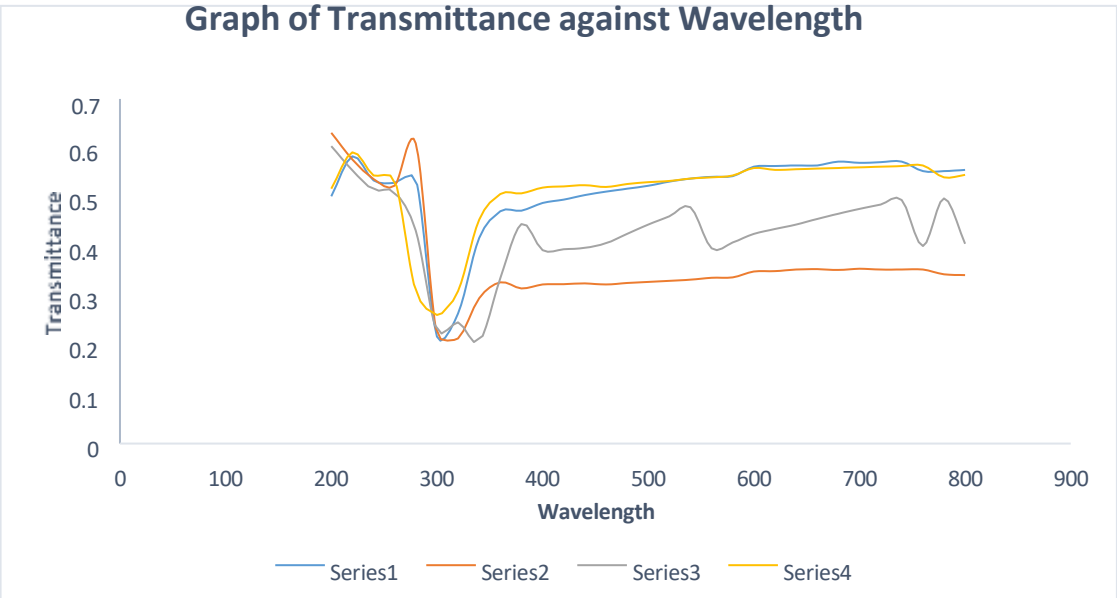


Fig 3.2: Transmittance versus wavelength for CuO-ZnO thin films at varying precursor concentrations

If you're making a window or a transparent electrode, you want your film to be see-through. The transmission spectra (Figure 3.2) shows us exactly that. Slide 1 (0.2M) displays the highest transmittance, peaking at approximately 59% in the visible region (550-700 nm). This high transparency correlates with its thinner film structure and lower material density, resulting in reduced light scattering and absorption. As precursor concentration increases, a progressive decrease in transmittance is observed: Slide 2 (0.4M): Moderate transmittance (~30-40%),

Slide 3 (0.6M): Minimal transmittance (~14%), representing the opaquest film, Slide 4 (0.8M): Slight increase in transmittance compared to Slide 3 (~20-25%).

The non-linear recovery of transmittance at 0.8M is an intriguing finding that warrants discussion. This phenomenon may result from structural changes at high concentrations. The wavelength-dependent transmission shows characteristic interference fringes, particularly evident in Slides 1 and 2, indicating smooth, uniform film surfaces with good optical quality. The presence of these fringes confirms the formation of coherent thin films suitable for optoelectronic applications. This tells us that lower concentrations are perfect for applications where you need transparency, while the mid-range is for when you want to block or absorb light.

Optical Thickness Spectra

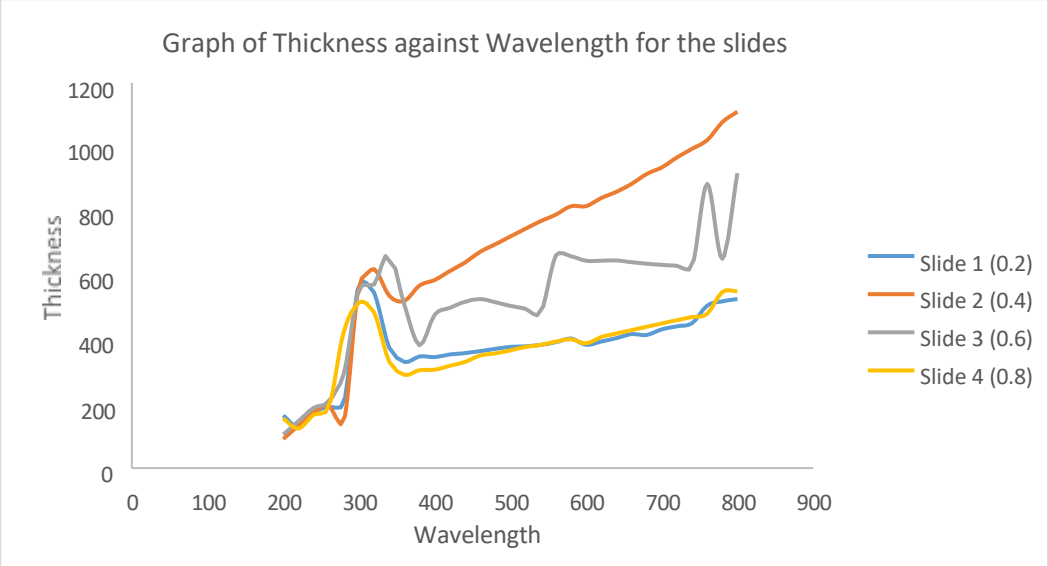


Fig 3.3: Film thickness versus wavelength for CuO-ZnO nanocomposite slides prepared at different concentrations.

The optical thickness measurements, derived from interference patterns in the transmission spectra, reveal a strong correlation between precursor concentration and film growth. The thickness values shown represent the wavelength-dependent optical path length, which combines both physical thickness and refractive index effects.

Slide 2 (0.4M) achieves the maximum thickness, exceeding 1100 nm across the visible spectrum (400-700 nm). This substantial thickness provides several advantages; Enhanced light absorption through increased interaction volume, Greater material loading for photocatalytic surface reactions, Improved mechanical stability of the film structure. The thickness progression follows an expected trend of increasing with concentration up to 0.4M, but the subsequent decrease at 0.6M and 0.8M suggests that film growth is not simply proportional to precursor availability.

The wavelength independence of thickness indicates that the films are optically homogeneous with minimal wavelength-dependent scattering, confirming good structural quality. The slight variations at shorter wavelengths (<400 nm) may result from increased absorption near the band edge affecting the interference pattern analysis.

Absorption Coefficient Squared Versus Photon Energy

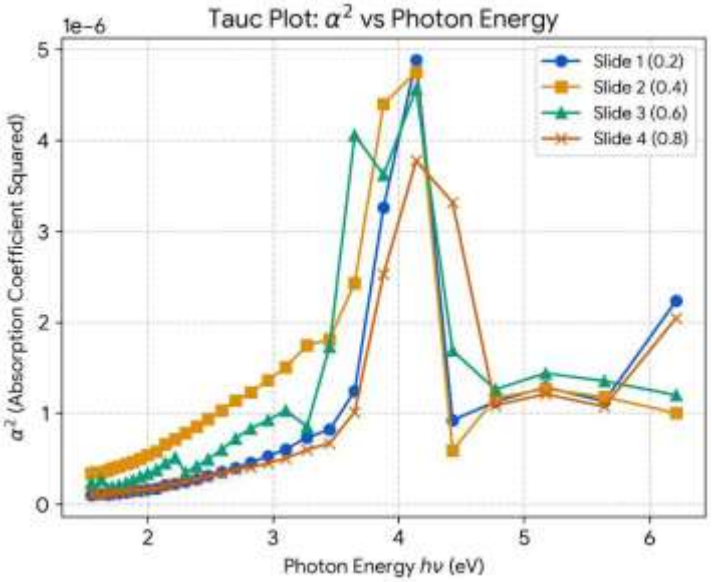


Fig 3.4 Tauc plots showing α² as a function of photon energy (hv) for CuO-ZnO thin films, used to determine optical bandgap energies

The Tauc plots represent the most critical analysis for understanding the electronic structure evolution with composition. The extrapolation of the linear region to the energy axis yields the direct optical bandgap values, revealing a striking non-monotonic trend:

Slide	Concentration	Bandgap (eV)	Optical Behavior
1	0.2M	3.5	UV-active, wide bandgap
2	0.4M	2.2	Visible-active, narrow bandgap
3	0.6M	2.8	Visible-UV intermediate
4	0.8M	3.3	Near-UV active

This bandgap variation represents successful bandgap engineering through compositional control, with the 0.4M composition achieving the narrowest bandgap (2.2 eV) a reduction of 1.3 eV from the 0.2M sample and 1.1 eV from pure ZnO (typically 3.37 eV).

The bandgap narrowing at 0.4M can be attributed to several phenomena such as formation of intermediate band states, quantum confinement effects, p-n junction formation while the increase in bandgap at higher concentrations (0.6M and 0.8M) suggests a transition in the dominant mechanism.

The 2.2 eV bandgap of Slide 2 is particularly significant for solar applications, as it closely matches the peak of the solar spectrum. This near-optimal bandgap, combined with high absorbance and thickness, positions the 0.4M composition as an exceptional candidate for thin-film photovoltaics. Conversely, the widest band gap for Slide 1 indicates its suitability for UV-related applications.

Conclusion

The observed trends are consistent with several earlier works: Wang *et al*. (2011) and Sue *et al*. (2010) both reported decreasing band gap with increasing CuO content, with optimal optical response near intermediate concentrations. He *et al.* (2011) highlighted an optimal CuO loading (~2 wt%) for maximum electrical conductivity, aligning with the performance of the

0.4M sample in this study. Vinodkumar *et al*. (2013) observed photoluminescence quenching with CuO doping, indicative of enhanced charge separation, supporting the improved absorbance and extinction coefficient at 0.4M. Dong *et al*. (2015) demonstrated that optimized shell thickness in core-shell CuO-ZnO nanostructures enhances charge separation, resonating with the increased film thickness and absorbance observed here.

The opto-electronic properties of the CuO-ZnO thin films demonstrate their versatility in several advanced applications. Based on the graphs and the experimental outcome, the samples correspond to the following concentrations:

The CuO-ZnO thin films demonstrated potential for various opto-electronic applications, each favoring specific concentrations based on their properties:

For solar cell applications, Sample 2 (0.4M) was found to be the most suitable. It exhibited the narrowest bandgap (2.2 eV), the highest absorbance, and optimal film thickness. These characteristics are essential for effective solar energy harvesting, as they enhance photon absorption and charge generation.

In the case of light-emitting diodes (LEDs), Sample 3 (0.6M) showed favorable behavior. With a moderately narrow bandgap of 2.8 eV and strong absorbance in the visible range, this sample holds promise for visible light emission applications.

For UV photodetectors and UV-filtering applications, Sample 1 (0.2M) was the most appropriate. It displayed the widest bandgap (3.5 eV) and the highest transmittance, both desirable for applications that require sensitivity to ultraviolet radiation or effective UV blocking.

In photocatalytic applications, which demand strong light absorption and efficient charge separation, Sample 2 (0.4M) again proved ideal due to its high absorbance, reduced bandgap, and thicker film structure—conditions that support enhanced catalytic activity under visible light.

Lastly, for transparent conducting oxide (TCO) uses, such as display coatings and transparent electrodes, Samples 1 (0.2M) and 4 (0.8M) are most appropriate. These films showed higher transmittance and thinner profiles, making them favorable for applications requiring optical transparency combined with electrical conductivity.

The concentration of CuO-ZnO in thin films plays a pivotal role in determining their opto-electronic behavior. The 0.4M composition demonstrated optimal performance across multiple metrics—absorbance, extinction coefficient, thickness, and bandgap—making it the most promising candidate for applications in solar energy conversion, photocatalysis, and LEDs. Lower concentrations, particularly 0.2M, are better suited for UV detection and transparent applications due to their higher transmittance and wider bandgap.

References

Borkar, T. *et al*. (2016). Effect of copper oxide addition on the sintering of zinc oxide. Ceramics International, 42(1), 416-422.

Dong, H. *et al*. (2015). Shape-controlled monoclinic CuO nanocrystals synthesized from Cu_2O octahedral nanocrystals and their selective detection of glucose in the presence of galactose and fructose. Dalton Transactions, 44(20), 9335-9342.

He, C. et al. (2011). Conductivity enhancement of electrospun CuO-ZnO nanofiber mats by doping with CO_3O_4 nanocubes. The Journal of Physical Chemistry C, 115(39), 19023-19030.

Kuo, S., Hsu, C., & Huang, M. (2013). Dye-sensitized solar cells using CuO-ZnO nanostructure composites as the photoanodes. Electrochimica Acta, 107, 650-655.

Özgür, Ü. *et al*. (2005). A comprehensive review of ZnO materials and devices. Journal of Applied Physics, 98(4), 041301.

Sue, K. *et al*. (2010). Effect of CuO doping on the optical properties of ZnO nanoparticles by sol–gel method. Advanced Powder Technology, 21(6), 618-624.

Vinodkumar, R. et al. (2013). Influence of copper oxide doping on the optical and electrical properties of ZnO thin films prepared by chemical spray technique. Superlattices and Microstructures, 64, 33-44.

Volanti, D.P. *et al*. (2013). The role of defects on the synthesis of copper oxide nanocubes by a hydrothermal method: morphological and optical properties. CrystEng Comm, 15(40), 8146-8152.

Wang, J. *et al*. (2011). Photocatalytic activity of CuO–ZnO nanostructures prepared via an electrochemical method. Superlattices and Microstructures, 49(4), 447-456. +6